CETRA[2016]

4th International Conference on Road and Rail Infrastructure
23–25 May 2016, Šibenik, Croatia

Road and Rail Infrastructure IV

Stjepan Lakušić – EDITOR

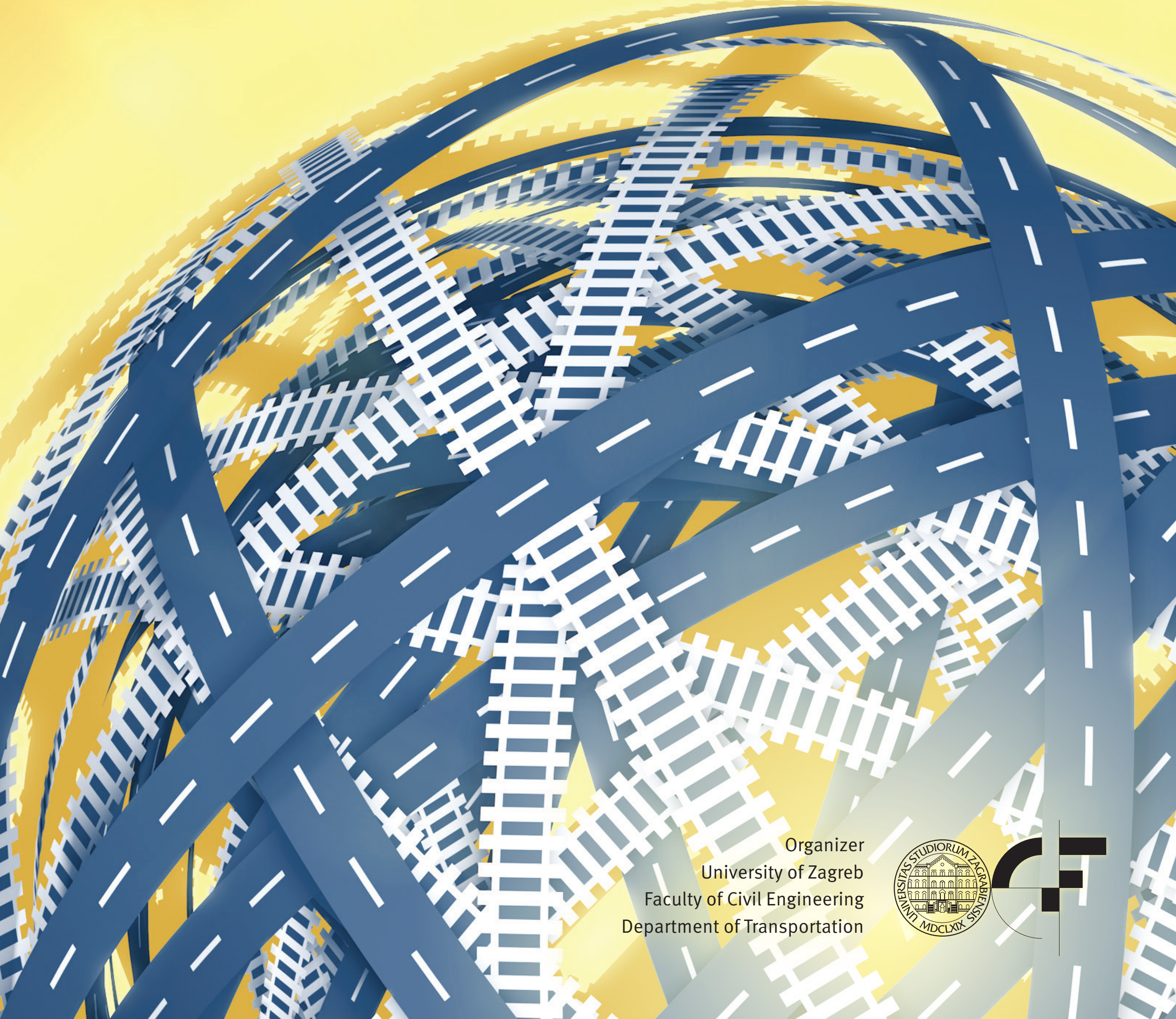

Organizer
University of Zagreb
Faculty of Civil Engineering
Department of Transportation

CETRA[2016]
4th International Conference on Road and Rail Infrastructure
23–25 May 2016, Šibenik, Croatia

TITLE
Road and Rail Infrastructure IV, Proceedings of the Conference CETRA 2016

EDITED BY
Stjepan Lakušić

ISSN
1848-9850

PUBLISHED BY
Department of Transportation
Faculty of Civil Engineering
University of Zagreb
Kačićeva 26, 10000 Zagreb, Croatia

DESIGN, LAYOUT & COVER PAGE
minimum d.o.o.
Marko Uremović · Matej Korlaet

PRINTED IN ZAGREB, CROATIA BY
"Tiskara Zelina", May 2016

COPIES
400

Zagreb, May 2016.

Proceedings of the
4th International Conference on Road and Rail Infrastructures – CETRA 2016
23–25 May 2016, Šibenik, Croatia

Road and Rail Infrastructure IV

EDITOR
Stjepan Lakušić
Department of Transportation
Faculty of Civil Engineering
University of Zagreb
Zagreb, Croatia

ORGANISATION

CHAIRMEN

Prof. Stjepan Lakušić, University of Zagreb, Faculty of Civil Engineering
Prof. emer. Željko Korlaet, University of Zagreb, Faculty of Civil Engineering

ORGANIZING COMMITTEE

Prof. Stjepan Lakušić
Prof. emer. Željko Korlaet
Prof. Vesna Dragčević
Prof. Tatjana Rukavina
Assist. Prof. Ivica Stančerić
Assist. Prof. Saša Ahac

Assist. Prof. Maja Ahac
Ivo Haladin, PhD
Josipa Domitrović, PhD
Tamara Džambas
Viktorija Grgić
Šime Bezina

All members of CETRA 2016 Conference Organizing Committee are professors and assistants of the Department of Transportation, Faculty of Civil Engineering at University of Zagreb.

INTERNATIONAL ACADEMIC SCIENTIFIC COMMITTEE

Davor Brčić, University of Zagreb
Dražen Cvitanić, University of Split
Sanja Dimter, Josip Juraj Strossmayer University of Osijek
Aleksandra Deluka Tibljaš, University of Rijeka
Vesna Dragčević, University of Zagreb
Rudolf Eger, RheinMain University
Makoto Fujiu, Kanazawa University
Laszlo Gaspar, Institute for Transport Sciences (KTI)
Kenneth Gavin, University College Dublin
Nenad Gucunski, Rutgers University
Libor Izvolt, University of Zilina
Lajos Kisgyörgy, Budapest University of Technology and Economics
Stasa Jovanovic, University of Novi Sad
Željko Korlaet, University of Zagreb
Meho Saša Kovačević, University of Zagreb
Zoran Krakutovski, Ss. Cyril and Methodius University in Skopje
Stjepan Lakušić, University of Zagreb
Dirk Lauwers, Ghent University
Dragana Macura, University of Belgrade
Janusz Madejski, Silesian University of Technology
Goran Mladenović, University of Belgrade
Tomislav Josip Mlinarić, University of Zagreb
Nencho Nenov, University of Transport in Sofia
Mladen Nikšić, University of Zagreb
Dunja Perić, Kansas State University
Otto Plašek, Brno University of Technology
Carmen Racanel, Technological University of Civil Engineering Bucharest
Tatjana Rukavina, University of Zagreb
Andreas Schoebel, Vienna University of Technology
Adam Szeląg, Warsaw University of Technology
Francesca La Torre, University of Florence
Audrius Vaitkus, Vilnius Gediminas Technical University

CETRA 2016 23–25 May 2016, Šibenik, Croatia
4th International Conference on Road and Rail Infrastructure

FLOW ON THE BALLASTED TRACKBED WITH PERMEABLE SURFACES AND ITS INFLUENCE ON THE BALLAST FLIGHT

Jianyue Zhu, Zhiwei Hu
University of Southampton, Faculty of Engineering and the Environment, Aerodynamics and Flight Mechanics Research Group, United Kingdom

Abstract

Related to the train underfloor carbody aerodynamics, a phenomenon of ballast flight occurs frequently associated with the operation of high-speed railways. Ballast flight will cause rail defect known as "ballast pitting" which is formed by the small ballast particles becoming trapped between the rail running surface and the vehicle wheels. Generally, the ballast particles have irregular shapes and are distributed on the trackbed which has a permeable surface. The flow developed beneath a high-speed train running on a ballasted track and around the ballast particles is turbulent and has strong influence on the ballast flight. This paper investigates the aerodynamic behaviour of the flow past the ballasted trackbed with permeable surfaces using computational fluid dynamics based on the delayed detached-eddy simulation. It is found that the flow field is highly unsteady due to strong flow separations and interactions developed around the gaps of the permeable surfaces. The ballast particles located on the permeable surfaces are situated in the stronger turbulent flow and are subject to larger fluctuating lift force than the particles located on solid surfaces. Moreover, the fluctuating lift, drag and side forces increase when the ballast particles are located beneath the bogie cavity area. When the ballast particles become airborne, the fluctuating forces generated around them increase greatly since the particles are situated in the unsteady flow with more flow interactions. Therefore, the stronger unsteady flow developed around the trackbed with a permeable surface will produce larger fluctuating forces on the ballast particles, which will be more likely to cause ballast flights for high-speed railways.

Keywords: ballast flight, flow behaviour, ballasted trackbed, permeable surface, aerodynamic forces

1 Introduction

High-speed rail networks are being developed rapidly around the world. Many investigations have been made to understand the aerodynamics of high-speed trains [1,2]. Related to the underfloor carbody aerodynamics, a phenomenon of ballast flight under normal meteorological conditions occurs more frequently and the railhead damage known as "ballast pitting" has become more popular associated with the operation of high-speed railways. This rail defect is formed by the small ballast particles becoming trapped between the rail running surface and the vehicle wheels. In order to understand the mechanism of the ballast flight, a full-scale field experiment was carried out to investigate the aerodynamic and mechanical forces acting on ballast particles which were generated during the passage of a high-speed train [3]. Moreover, an analytical model was established to identify the factors causing the small ballast particles being ejected from the trackbed. It was found that ballast flight could arise from a combination of aerodynamic and mechanical effects and the process was stochastic [3]. The basic charac-

teristics of the flow between the underbody of a high-speed train and the ground have been studied numerically based on a turbulent Couette flow model to simplify the calculation [4]. Results showed that an equivalent roughness of the trackbed made of sleepers and ballast could be obtained based on this analytical method. Additionally, a full-scale numerical simulation of the ICE3 (inter-city express) geometry based on Reynolds-averaged Navier-Stokes investigation together with a wall function approach was performed. It was found that the boundary layer was developed considerably in the train underfloor region due to the generation of turbulence and secondary flow in the vicinity of the bogies. Moreover, the skin friction was increased significantly immediately downstream of the inter-car gap. It was pointed out by the authors that these numerical results were needed to improve confidence by grid independence study as they didn"t correspond well with the experimental measurements [5].
The mechanisms of the ballast flight are still not well understood [3, 5]. The flow beneath a high-speed train running on a ballasted track is highly unsteady and has strong influence on the behaviour of the ballast flight. Generally, ballast particles have irregular shapes and are distributed adjacent to the other ballast particles on the trackbed; thus the small gaps are formed between the ballast particles, which can be modelled as particles located on a permeable surface. This paper aims to investigate the aerodynamic behaviour of the flow past the ballasted trackbed with permeable surfaces using the numerical simulations.

2 Numerical method

Aerodynamically, high-speed trains are operating within the low Mach number flow regime, for example at 300 km/h the Mach number is about 0.25. The incoming flow (30 m/s) simulated in this paper is at a low Mach number of 0.09 and thereby the compressibility effects on hydrodynamic airflow field are small and thus can be neglected. Therefore, the unsteady, incompressible Navier-Stokes equations are used to solve the flow field. The continuity and momentum equations in tensor notation are given by:

$$\frac{\partial u_i}{\partial x_i} = 0 \tag{1}$$

$$\frac{\partial u_i}{\partial t} + u_j \frac{\partial u_i}{\partial x_j} = f_i - \frac{1}{\rho}\frac{\partial p}{\partial x_i} + \nu \frac{\partial^2 u_i}{\partial x_j \partial x_j} \tag{2}$$

where x_i represents the Cartesian coordinates in the streamwise, crossflow and vertical directions for i = 1, 2, 3. p is the pressure, ρ is the density, ν the kinematic viscosity, f_i is the body force and u_i the flow velocity components. Here ρ and ν are constants for incompressible flow. The open source software OpenFOAM-2.2.1 is employed to solve the governing equations numerically. A second-order accuracy scheme is utilized for the convection and diffusion terms of the spatial derivatives and the temporal discretization follows a second-order fully implicit scheme. The pressure-velocity algorithm PIMPLE, combining PISO (pressure implicit with splitting of operator) and SIMPLE (semi-implicit method for pressure-linked equations) algorithms, is applied to solve iteratively the resulting discretized linear-algebra equation system. The delayed detached-eddy simulation (DDES) model based on the Spalart-Allmaras turbulence model is employed for the current flow calculations [6].

3 Simulation setup

The three-dimensional models of ballasted trackbed with permeable surfaces and ballast particles used in this study are displayed in Figure 1. The ballast particles have dimensions of 10 mm, 10 mm and 5 mm in the streamwise, spanwise and vertical directions, respectively

and are connected to the trackbed on the four corners with an area of 2 mm × 2 mm. The width and depth of the gap of the permeable surface are 6 mm and 5 mm. The junction area of the gaps without the ballast particles are filled by the blocks with dimensions of 6 mm × 6 mm × 5mm along the streamwise, spanwise and vertical directions, respectively. The length of the ballastbed is 0.4 m corresponds to the gap between two adjacent sleepers in reality. There are four cases simulated here: the “case1” represents the case of all particles attached on the permeable surface (Figure 1a); to change the ballast surface around the particle “C1” to solid and have the same incoming flow from the permeable surface, the “case2” is built as shown in Figure 1 (b); based on the “case2”, the “case3” has a gap of 2 mm between the particle “C1” bottom and the trackbed top surface; with the bogie cavity added to the “case1”, the “case4” is used to investigate the influence of train undercarriage turbulent flow and sketched in Figure 1 (c) with the main dimensions.
Based on the grid convergence study for a cylinder case [7,8], a fully block-structured mesh is generated around all the geometries. The first point is set as 1×10^{-5} m from the wall surfaces and grows at a ratio of 1.1 inside the boundary layer. This yields a maximum value of y^+ (the dimensionless first-cell spacing, $y^+ = yu_\tau/\nu$ where y is the distance from the wall, u_τ the friction velocity and ν kinetic viscosity) less than 1 for all cases to ensure that the boundary layer is resolved properly and the turbulence model employed can account for the low-Reynolds number effects inside the viscous sublayer. This grid generation strategy results in a total number of grid points of 33.2 million in the entire domain for the “case1”; 32.3 million for the “case2”; 33.3 million for the “case3”; and 39.1 million for the “case4”. For the case of permeable surfaces around the ballast particle “C1” (“case1”), another coarse mesh with 19.6 million grid points was also used for simulations and the results from the two meshes with different resolutions were very close (the discrepancies in root-mean-square (RMS) and mean values of aerodynamic force coefficients for the ballast particle “C1” are less than 7%.), as shown in Table 1. The meshes with fine resolution will be used for all the simulations.

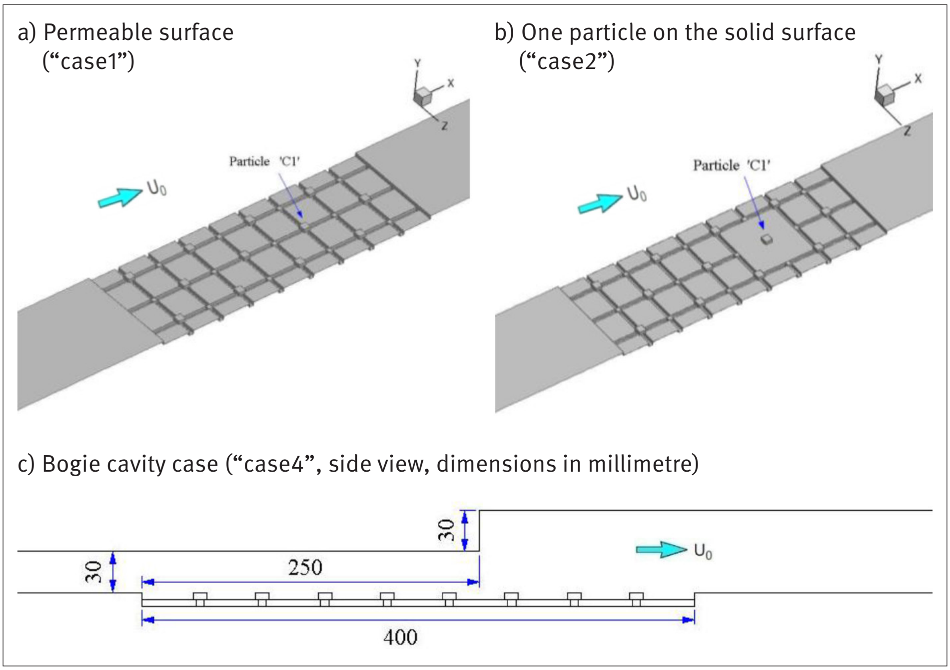

Figure 1 Simplified models of ballasted trackbed with permeable surfaces

Table 1 Root-mean-square and mean values of aerodynamic force coefficients for the ballast particle "C1"

		Coarse mesh	Fine mesh	Discrepancy
RMS value	Fluctuating lift	0.5486	0.5143	6.67%
	Fluctuating drag	0.4507	0.4222	6.75%
	Fluctuating side force	0.3398	0.3186	6.65%
Mean value	Lift coefficient	1.602	1.5415	3.92%
	Drag coefficient	2.7142	2.7157	0.06%
	Side force coefficient	-0.0938	-0.0942	0.43%

The boundary conditions applied are as follows: the upstream inlet flow is represented as a steady uniform flow of 30 m/s (U_0) with a low turbulence intensity. The side boundaries are specified as periodic boundary conditions; a pressure outlet with zero gauge pressure is imposed at the downstream exit boundary; all solid surfaces are defined as stationary no-slip walls. Simulations are run with a physical timestep size of 1×10^{-6} s initially and then followed by 2×10^{-6} s which gives an adequate temporal resolution for the implicit time marching scheme used with a Courant-Friedrichs-Lewy (CFL) number of less than 1 within the whole computational domain.

4 Simulation results

In order to understand the flow behaviour around the ballast particles located on the ballasted trackbed with the permeable surfaces, the calculation results of the instantaneous iso-surfaces of Q-criterion and the velocity fields are displayed to get an overview of the unsteady flow developed around the geometries; then, the fluctuating force coefficients of ballast particles are compared for different cases.

4.1 Instantaneous flow field

The flow structures developed around the permeable surfaces ("case1"), represented by the iso-surfaces of the normalized Q-criterion at the level of 1 (based on $Q/[(U_0/l)^2]$, where l is the particle length of 10 mm) are visualized in Figure 2. They are coloured by the non-dimensional velocity magnitude. It can be seen that various scales of vortices are formed along the gaps of the permeable surfaces as different flow interactions occur there. Moreover, a higher level of flow-field unsteadiness is developed around the leading edge of the rear sleeper where the strong flow impingements are generated.

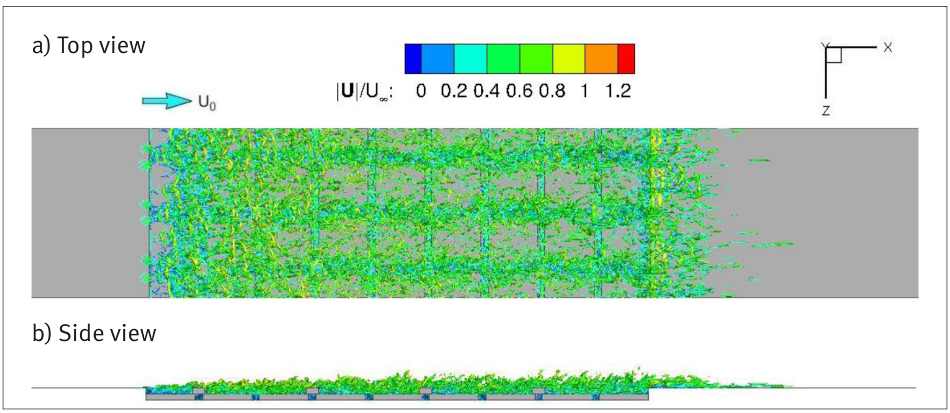

Figure 2 Iso-surfaces of the instantaneous normalized Q-criterion

Figure 3 shows the flow structure developed around the permeable surfaces beneath the bogie cavity (“case4”), represented by the iso-surfaces of the normalized Q-criterion at a level of 0.5. It shows that a shear layer is developed from the cavity leading edge, and bent upwards in the streamwise direction. This shear layer travels downstream and interacts strongly with the flow developed in the bogie cavity. Subsequently, all vortices are mixed up and impinge on the upper wall of the cavity, leading to the unsteady flow with complex structure formed there. Figure 4 shows the instantaneous velocity field in vertical mid-span (“case4”). It can be seen that the shear layer developed from the cavity leading edge also has a strong interaction with the flow developed on the ballasted trackbed. Thus, a highly unsteady flow is formed between the bogie cavity and the trackbed. This makes ballast particles subject to stronger unsteady aerodynamic forces, which could lead to ballast flight happen.

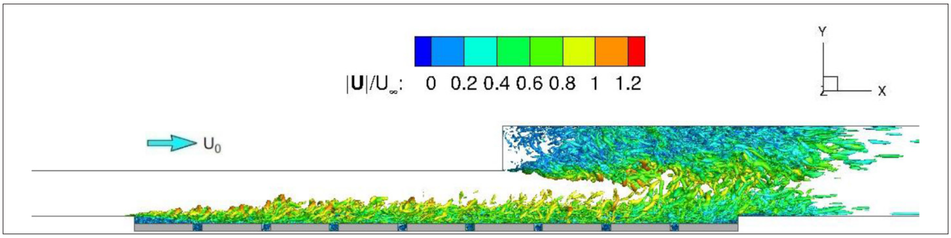

Figure 3 Iso-surfaces of the instantaneous normalized Q-criterion (side view)

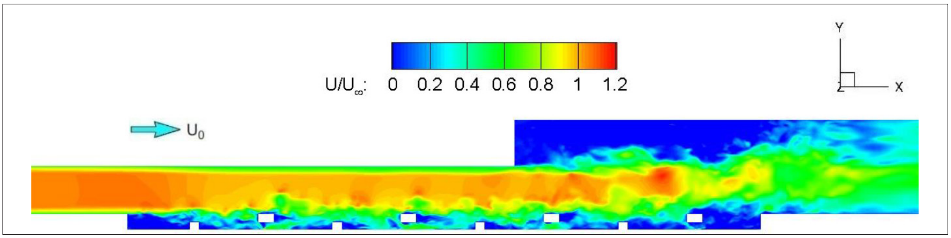

Figure 4 Contours of instantaneous velocity in vertical mid-span (side view)

Figure 5 shows the instantaneous velocity field at the ballast particle horizontal mid-plane from a top view in the bogie cavity case (“case4”). It can be seen that the flow separation occurs at the side edge of the ballast particle. The vortices formed in the front ballast particles” wake are convected downstream and impinge on the rear ballast particles, causing more flow interactions around these regions and generating the unsteady flow along the trackbed.

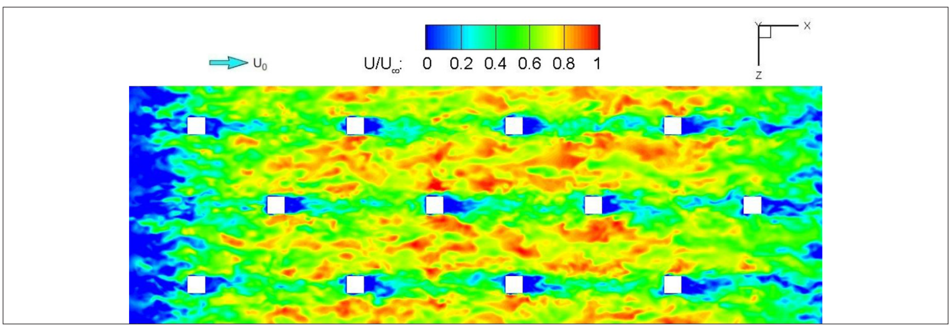

Figure 5 Contours of instantaneous velocity through the ballast particle horizontal mid-plane (top view)

4.2 Fluctuating forces on ballast particles

The comparisons of the root-mean-square fluctuating lift, drag and side force coefficients for one ballast particle (particle "C1" shown in Figure 1) of various cases, from the "case1" to the "case4" as described earlier, are presented in Figure 6. By comparing the results from the "case1" and the "case2", it is found that the RMS value of the fluctuating lift force is higher while those of the drag and side forces are slightly lower when the particle is located on the permeable surface of the trackbed, making the ballast flight apt to occur. When the particle becomes airborne ("case3"), the fluctuating force, especially the lift force increases greatly compared to the particle attached to the permeable surface of the trackbed ("case1"). This is because when the ballast particle leaves the trackbed, it is situated in a more energetic turbulent flow, and thus strong flow interactions are developed around all surfaces of the particle and generate the high force fluctuations on it. Moreover, based on the comparisons between the "case4" and the "case1", results show that all the forces increase as the ballast particles distributed beneath the bogie cavity where the unsteady flow development is relatively stronger, as discussed earlier. Therefore, the fluctuating forces generated on the ballast particles are directly affected by the turbulent flow developed around them. The unsteady flow generated around the region between the train underbody and the permeable ballasted trackbed will induce large fluctuating forces on the ballast particles situated within it and make the ballast flight more likely to happen.

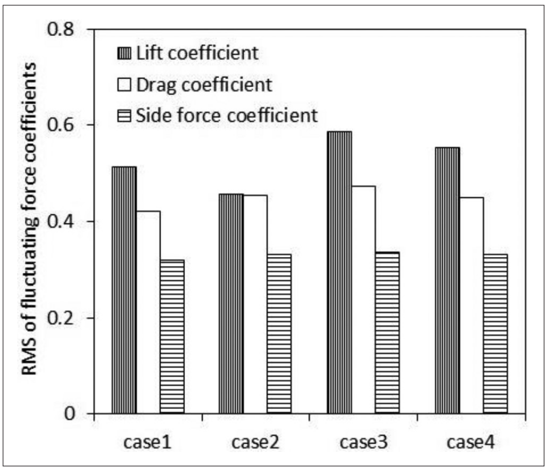

Figure 6 Root-mean-square of fluctuating force coefficients of ballast particles

5 Conclusions

The aerodynamic behaviour of the flow past the ballast particles on the permeable ballasted track and beneath the bogie cavity has been investigated using delayed detached-eddy simulation. Results show that compared to the particles attached on a solid surface, the ballast particles located on the permeable surfaces are situated in various flow interactions and are subject to larger fluctuating lift force. Moreover, when the permeable ballasted trackbed is located beneath the bogie cavity, a shear layer developed from the cavity leading edge has a strong interaction with the flow developed from the bogie cavity and the trackbed. All vortices are mixed up and convected downstream and a highly unsteady flow is generated due to the strong flow interactions occurring there. Thus, the larger fluctuating forces are induced on the ballast and make the ballast flight happen easily. When the ballast particles become

airborne, the fluctuating lift force increase greatly since the particles are situated in the more energetic turbulent flow.
Note that in reality the turbulent inflow and more detailed geometries present will lead to more complex flow structures and this will affect the induced forces on the ballast particles around the trackbed. The pressure pulse generated from the approaching train coupled with the severe mechanical vibration of the trackbed may play a key role in the initiation of ballast flight. The large turbulent fluctuations around the vehicle nose, inter-car gaps and tail region are apt to making the ballast particles airborne. All these factors need to be accounted for in the future work.

Acknowledgements

This project was supported under the auspice of the Engineering and Physical Science Research Council (EP/K03765X/1). The numerical simulations were performed on the Iridis4 cluster managed by the University of Southampton.

References

[1] Baker, C. J.: The flow around high speed trains. Journal of Wind Engineering and Industrial Aerodynamics, 98, pp. 277-298, 2010.

[2] Schetz, J. A.: Aerodynamics of high speed trains. Annual Review of Fluid Mechanics, 33, pp. 371-414, 2001.

[3] Quinn, A. D., Hayward, M., Baker, C. J., Schmid, F., Priest, J. A., Powrie, W.: A full-scale experimental and modelling study of ballast flight under high-speed trains. Proceedings of the Institution of Mechanical Engineers Part F, Journal of Rail and Rapid Transit, 224, pp. 61-74, 2009.

[4] García, J., Crespo, A., Berasarte, A., Goikoetxea, J.: Study of the flow between the train underbody and the ballast track. Journal of Wind Engineering and Industrial Aerodynamics, 99, pp. 1089-1098, 2011.

[5] Kaltenbach, H.-J., Gautier, P.-E., Agirre, G., Orellano, A., Schroeder-Bodenstein, K., Testa, M., Tielkes, T.: Assessment of the aerodynamic loads on the trackbed causing ballast projection: results from the DEUFRAKO project aerodynamics in open air (AOA). Proceedings of the World Congress on Rail research, South Korea, 2008.

[6] Spalart, P.R., Deck, S., Shur, M.L., Squires, K.D., Strelets, M.Kh., Travin, A.K.: A new version of detached-eddy simulation, resistant to ambiguous grid densities. Theoretical and Computational Fluid Dynamics, 20, pp. 181-195, 2006.

[7] Zhu, J.Y., Hu, Z.W., Thompson, D.J.: Flow behaviour and aeroacoustic characteristics of a simplified high-speed train bogie. Proceedings of the Institution of Mechanical Engineers Part F: Journal of Rail and Rapid Transit, Published online September 30, 2015.

[8] Zhu, J.Y.: Aerodynamic Noise of High-speed Train Bogies. PhD Thesis. University of Southampton, 2015.